Observation of nonlinear sloshing induced by wetting dynamics

Guillaume Michel, François Pétrélis, Stéphan Fauve

HAL Id: hal-01493943
https://hal.sorbonne-universite.fr/hal-01493943

Submitted on 22 Mar 2017

Observation of nonlinear sloshing induced by wetting dynamics

Guillaume Michel,* François Pétrélis, and Stéphan Fauve

Laboratoire de Physique Statistique, École Normale Supérieure, CNRS,
Université P. et M. Curie, Université Paris Diderot, Paris, France

(Dated: March 20, 2017)

Back-and-forth oscillations of a container filled with fluid often result in spilling as the gravest mode gets excited, a well-known phenomenon experienced in everyday life and of particular importance in industry. Our understanding of sloshing is largely restricted to linear response, and existing extensions mostly focus on nonlinear coupling between modes. Linear theory is expected to correctly model the dynamics of the system as long as the amplitude of the mode remains small compared to another length scale, so far unknown. Using a fluid in the vicinity of its critical point, we demonstrate that in perfect wetting this length scale is neither the wavelength nor the capillary length but a much shorter one, the thickness of the boundary layer. Above this crossover length scale, the resonance frequency remains roughly constant while dissipation significantly increases. We also show that dynamical wetting is involved in both linear and nonlinear dissipative processes.

Introduction.— Although the study of sloshing in the simplest configuration of a cylindrical container can be traced back to Poisson at the beginning of the 19th century [1], a significant gap still exists between theory and experiments even for the linear response of the gravest mode. While effective devices have long been investigated to prevent excessive surface deformations, the most famous ones being antislosh baffles (see Ref. [2] for a review), sloshing control could be improved by understanding the precise dissipative processes resulting from back-and-forth displacements of a container. Moreover, the limit of linear theory is unknown: If we were asked if a linear damping correctly describes the oscillations taking place in a cup of coffee, many of us would hesitate before giving an opinion. The associated damping time scale computed from linear theory is more than 10 s [3], thus providing a strong hint that nonlinearities occur. In this Rapid Communication, we evidence that dynamical wetting processes contribute to linear damping and that such linear theory is restricted in perfect wetting to oscillations smaller than the thickness of the boundary layer (a fraction of a millimeter in the case of a cup of coffee).

The characteristics of the gravest mode for an inviscid, irrotational, and incompressible flow with a free surface can be found in many textbooks (*e.g.*, Refs. [2, 4]). Natural frequency computed in this framework differs from the experimental values from less than 1% [5, 6] up to around 10% [7–9]. In contrast, measurements of damping are associated with larger discrepancies: a theory based on dissipation localized in bottom and wall boundary layers underestimates experimental dissipation from a few percent [7] to as much as a few hundred percent [5, 8, 9]. These disparities have been ascribed to both surface contamination and capillary effects close to the contact line.

It is common knowledge that a free surface quickly gets polluted unless care is taken to avoid it: full contamination occurs within an hour for water and significantly increases the damping of surface waves [10]. This correction to the natural frequency and to the damping has been first computed in circular geometry by Miles [11], with Marangoni elasticity having been later added in some limit by Nicolás and Vega [12]. Even though it is clearly an efficient damping mechanism, the exact values of these corrections strongly depend on chemical properties (*e.g.*, solubility of the contaminant or Marangoni elasticity of the film) whose measurements are difficult.

Dissipation caused by the motion of the meniscus has also been studied theoretically, by considering the work of capillary forces (those involved in the equilibrium Young contact angle). This has been first achieved by Miles for various wetting configurations [11, 13]. Experiments show that a meniscus strongly increases dissipation [14], the damping being maximal for zero contact angle [15]. However, dissipation considered in these theoretical studies vanishes for perfect wetting. In addition, we note that the computation of viscous energy loss in a meniscus undergoing an oscillating motion is still an open problem.

In the present experiment, we measure the natural frequency and damping of the first sloshing mode in a cylindrical container. Using a fluid in the vicinity of the liquid-vapor critical point allows a continuous modification of physical parameters involved in the sloshing dynamics and provides a better control of surface contamination and wetting properties. Standard linear theory is found to accurately describe the natural frequency, whereas it clearly underestimates the damping. Since the surface is clean and the wetting is perfect, this provides a measurement of viscous energy dissipation in the contact line. The nonlinear dynamics of this oscillator is also addressed by tuning the forcing amplitude: We report that the first nonlinearity to arise is a damping enhancement that we attribute to the wetting dynamics. We demonstrate that the crossover between linear and nonlinear dynamics occurs when the amplitude becomes of the order of the thickness of the boundary layer, a surprisingly small characteristic length.

Experimental setup.— The experimental setup is sketched in Fig. 1 and consists of a cylindrical container of radius $R = 50$ mm and height $2h = 25$ mm filled with SF_6 of purity $> 99.97\%$. The total density ρ has been set close to the critical density ρ_c so that in the vicinity of the critical point the liquid and gas phases have the same volume, the height of the liquid being therefore $h = 12.5$ mm. The pressure P and the temperature T inside the cell are measured with a Kistler 4500B pressure sensor and a Pt100 resistance thermometer: the relation $P(T)$ in the supercritical domain with the data from Ref. [16] leads to $\rho = 720$ kg.m^{-3}. This container is surrounded by a Lauda Master thermostated bath, making temperature fluctuations less than 0.01 K. Four windows allow the observation of the surface motion: two lateral ones of radius 5 mm, and two on the upper and lower surfaces of radius 20 mm.

The entire device is subjected to a harmonic horizontal translation $\Delta X \cos(\omega t + \phi)$ imposed by a BK 4809 vibration exciter. The actual displacement is measured by a noncontact Electro Corp sensor and processed by a SR 830 lock-in amplifier that gives access to ΔX and ϕ. A laser aligned with and close to the cylinder axis is deflected at the liquid-vapor interface and the motion of the beam along the translational direction, $R_{las} \cos(\omega t + \theta_{las})$, is tracked by a UDT 301-DIV position sensing detector. This signal is handled by a similar lock-in amplifier: R_{las}, ΔX, θ_{las} and ϕ are finally recorded with a NI-acquisition card. For a given forcing amplitude ΔX, the sloshing dynamics is therefore characterized by the amplitude and phase responses, respectively R_{las} and $\theta_{las} - \phi$.
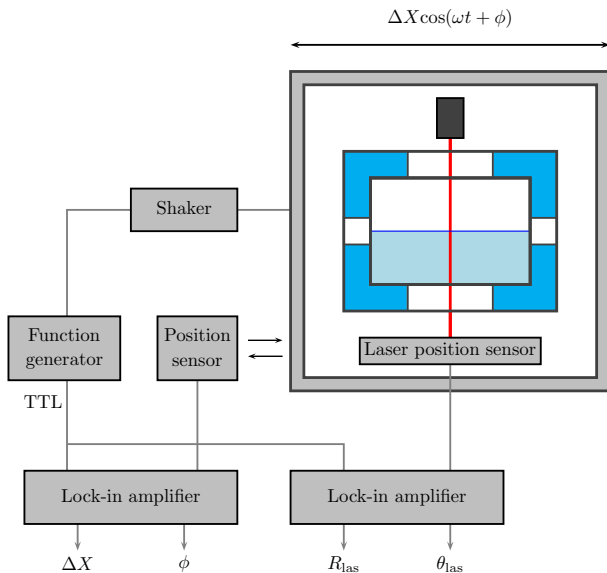

FIG. 1. Experimental setup

The liquid and vapor densities (resp. $\rho_{(\ell)}$ and $\rho_{(v)}$), the refractive indices (resp. $n_{(\ell)}$ and $n_{(v)}$) and the surface tension σ evolve close to the critical temperature T_c

according to

$$
\begin{cases}
\rho_{(\ell)} = \rho_c(1 + B_0\epsilon^\beta), & \rho_{(v)} = \rho_c(1 - B_0\epsilon^\beta) \\
n_{(\ell)} = n_c(1 + A_0\epsilon^\beta), & n_{(v)} = n_c(1 - A_0\epsilon^\beta) \\
\sigma = \sigma_0\epsilon^\mu
\end{cases}
\tag{1}
$$

where $\epsilon = (T_c - T)/T_c$ is the dimensionless distance to the critical point, n_c is the refractive index of the supercritical phase and $(\beta \simeq 0.325, \mu \simeq 1.26)$ are critical exponents. In our experiment $T_c = (318.782 \pm 0.004)$K and ϵ has been tuned from 10^{-1} to 10^{-3}. Close to the critical point, the kinematic viscosities $\nu_{(\ell)}$ and $\nu_{(v)}$ verify $\nu_{(\ell)} \simeq \nu_{(v)} \simeq \nu \simeq 5.7 \ 10^{-8}$ m^2.s^{-1} [17].

Dynamics of the first sloshing mode.— Gently increasing ω for a fixed displacement ΔX reveals a large number of resonances, and we thereafter focus on the first one. The amplitude of this mode $\bar{\eta}_{1,1}(t)$ is expected to be modeled for small forcing amplitudes by a damped harmonic oscillator equation, that is

$$
\frac{d^2\bar{\eta}_{1,1}}{dt^2} + \left(\frac{\omega_{1,1}}{Q}\right)\frac{d\bar{\eta}_{1,1}}{dt} + \omega_{1,1}^2\bar{\eta}_{1,1} = \mathcal{F}(t),
\tag{2}
$$

where $\omega_{1,1}$ is the angular resonance frequency, $\omega_{1,1}/(2\pi Q)$ is the linear bandwidth and $\mathcal{F}(t)$ is the external driving force. For a lateral excitation $\Delta X \cos(\omega t + \phi)$, $\mathcal{F}$ comes from the difference of inertial accelerations between the two phases and scales as

$$
\mathcal{F} \propto \frac{\rho_{(\ell)} - \rho_{(v)}}{\rho_{(\ell)} + \rho_{(v)}}\Delta X \omega^2 \cos(\omega t + \phi).
\tag{3}
$$

The two characteristics of this oscillator that are $(\omega_{1,1}/Q)$ and $\omega_{1,1}$ are experimentally measured for a given displacement ΔX from a linear fit of the phase response close to the resonance, where [18]

$$
\theta_{las} - \phi \simeq -\frac{\pi}{2} - 2\frac{Q}{\omega_{1,1}}(\omega - \omega_{1,1}).
\tag{4}
$$

Typical plots of $(\theta_{las} - \phi)$ for a fixed temperature ($\epsilon = 0.017$) as a function of the forcing frequency $f = \omega/(2\pi)$ are reported in Fig. 2. They exhibit a nonlinear behavior since data for different forcing amplitudes do not coincide.

The addition of a quadratic nonlinearity in the dissipation correctly models all experimental data and we consider instead of (2) an oscillator equation of the form

$$
\frac{d^2\bar{\eta}_{1,1}}{dt^2} + \frac{\omega_{1,1}}{Q}(1 + C_{NL}\bar{\eta}_{1,1}^2)\frac{d\bar{\eta}_{1,1}}{dt} + \omega_{1,1}^2\bar{\eta}_{1,1} = \mathcal{F}(t). \tag{5}
$$

A straightforward analysis reveals that for such an oscillator, the lowest order correction to (4) reduces to a modification of the slope as the forcing increases, such that

$$
2\frac{Q}{\omega_{1,1}} \Rightarrow 2\frac{Q}{\omega_{1,1}}\left(1 - \frac{C_{NL}\mathcal{F}^2 Q^2}{4\omega_{1,1}^2}\right).
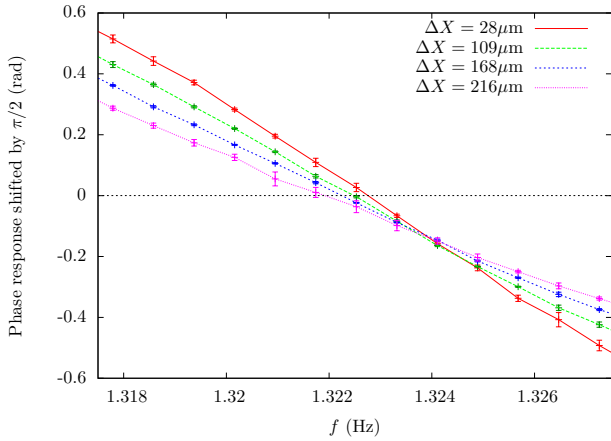\tag{6}
$$

FIG. 2. Typical phase evolution close to resonance ($\epsilon = 0.017$)

For the temperature considered in Fig. 2, we extract from linear fits of the phase response the resonance frequency (when $\theta_{\text{las}} - \phi = -\pi/2$) and the slope of these lines, see Fig. 3. Whereas the resonance frequency can be reasonably considered as constant, the slope has a clear dependence on the square of the forcing amplitude: for all considered temperatures, the relative variation of the slope reaches 100% before the variation of the frequency gets to 1%.
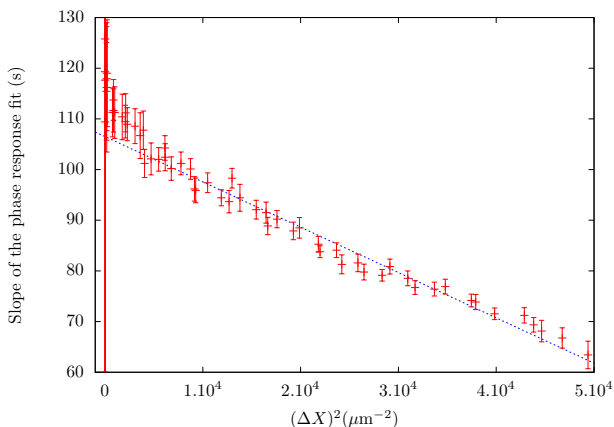

FIG. 3. Evolution of the phase close to resonance as a function of the displacement ΔX ($\epsilon = 0.017$)

For each temperature, we therefore have a direct measurement of the resonance frequency $\omega_{1,1}/(2\pi)$, the linear bandwidth $\omega_{1,1}/(2\pi Q)$ and the linear amplitude response at resonance G defined by $R_{\text{las}} = G\Delta X$ for small amplitudes (obtained by a direct fit of R_{las}, similar to the one in Fig. 3, not reported here for brevity). From the slope of the fit in Fig. 3, we also have access to the nonlinear coefficient $C_{\text{NL}}^{\Delta X}$, such that at the lowest order

$$1 + C_{\text{NL}}\bar{\eta}_{1,1}^2 = 1 + C_{\text{NL}}^{\Delta X}(\Delta X)^2. \tag{7}$$

Discussion. — In the linear potential theory of surface waves, the surface elevation $\eta(r, \theta, t)$ can be decomposed

into a sum of modes of the form [2, 4]

$$\bar{\eta}_{n,m}(t) \frac{J_m(k_{n,m}r)}{J_m(k_{n,m}R)} \cos(m\theta + \theta_{n,m}), \tag{8}$$

where J_m is the Bessel function of order m, $\theta_{n,m}$ is a constant that can be removed by considering independent sine and cosine functions of $m\theta$, $k_{n,m}$ is the wave-number (such that $k_{n,m}R$ is the nth root of J'_m) and $\bar{\eta}_{n,m}(t)$ is a harmonic function of frequency

$$f_{n,m} = \frac{1}{2\pi}\sqrt{\left(\frac{\rho_{(\ell)} - \rho_{(v)}}{\rho_{(\ell)} + \rho_{(v)}}\right)gk_{n,m}\tanh(k_{n,m}h)}. \tag{9}$$

The derivation of (9) assumes that both phases have the same height h and that surface tension can be ignored. Since we restrict this study to the mode of lowest frequency, corresponding to $m = n = 1$, this last assumption is valid. Close to the critical point, using (1), (9) reduces to $f_{1,1} = C\epsilon^{\beta/2}$, where C is a constant that depends on g, h, $k_{1,1} = 1.8412/R$ and B_0 ($B_0 = 1.62$ for SF_6 [19]). This accurately describes our experimental data, cf. Fig. 4. Minor corrections to (9) resulting from the damping or the wetting conditions exist (see, *e.g.*, [13]) but they are less than the uncertainty on B_0 and can therefore not be determined here.
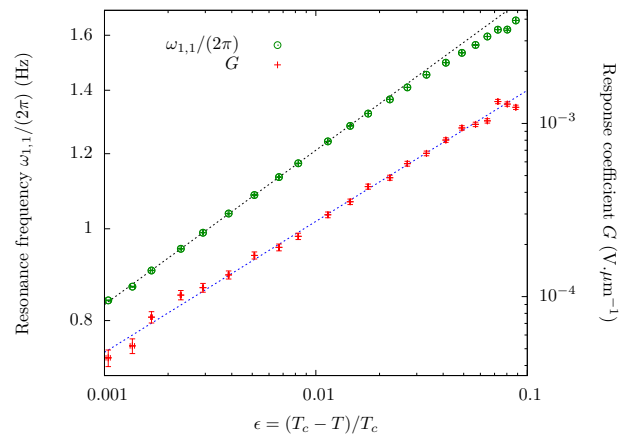

FIG. 4. Critical behavior of G and $\omega_{1,1}/(2\pi)$. One straight line is the theoretical prediction for $\omega_{1,1}/(2\pi)$ and the other one is a power-law fit of G of critical exponent 0.756.

We also checked that G has the correct scaling versus ϵ: stating that the displacement of the laser is related to the refraction indices and that at resonance the forcing term is fully balanced by dissipation, we get

$$R_{\text{las}} \propto \Delta n\bar{\eta}_{1,1} \propto \Delta n\frac{Q}{\omega_{1,1}}\omega_{1,1}\Delta\rho\Delta X. \tag{10}$$

Assuming that $\omega_{1,1}/Q \propto \epsilon^{\beta/4}$ (see below), G is directly related to ϵ via

$$G \propto \epsilon^{\beta-\beta/4+\beta/2+\beta} \propto \epsilon^{9\beta/4}. \tag{11}$$

Fitting our data with $G \propto \epsilon^{\exp}$ (see Fig. 4) leads to a critical exponent 0.756 ± 0.009, compatible with $9\beta/4 \simeq 0.731$.

We now consider the dissipative term, whose computation relies on an expansion on the small parameter $\delta k_{1,1}$, where $\delta = \sqrt{\nu/\omega_{1,1}}$ is the thickness of the viscous boundary layers. The very small kinematic viscosity of fluids close to the critical point (a few times $10^{-8}\mathrm{m}^2.\mathrm{s}^{-1}$) compared to the ones of more usual fluids (1.10^{-6} for water) makes this parameter small enough not to consider second order contributions (as bulk dissipation), that can be of importance otherwise [20]. If neither surface contamination nor capillary effects close to the meniscus are considered, damping thus reduces to the contributions of top, bottom and lateral boundary layers and [7]

$$\frac{\omega_{1,1}}{Q} = \frac{1}{R}\sqrt{\frac{\nu\omega_{1,1}}{2}}\left(1.84 + 3.68\frac{1 - h/R}{\sinh(3.68h/R)}\right). \quad (12)$$

Note that although this expression has been derived in [7] in the absence of gas, it also describes the present experiment given that phases have almost the same height and kinematic viscosity. Equation (12) predicts $\omega_{1,1}/(2\pi Q) = 9.5\epsilon^{0.081}$ mHz, while a fit of our data leads to $\omega_{1,1}/(2\pi Q) = (24.3 \pm 0.2)\epsilon^{0.074\pm0.002}$ mHz, cf. Fig. 5. This indicates that other first order dissipative terms (all in $\epsilon^{0.081}$) have to be considered.
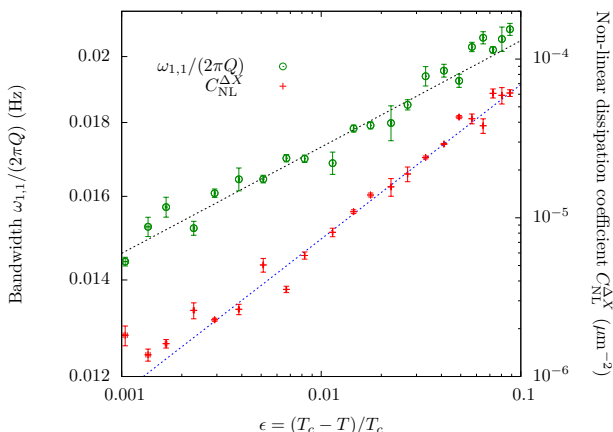

FIG. 5. Critical behavior of the linear and nonlinear damping. Straight lines are power-law fits with critical exponents 0.074 and 0.972.

Such terms could result from surface contamination, but we regard this possibility as unlikely. Indeed, the gathering of contaminants close to the interface results from a sizable surface tension σ, and σ vanishes at the critical point (for the range of temperature considered, $\sigma < 0.2$ mN.m^{-1} [17]). Dissipation caused by capillary forces at the meniscus could also be a guess, but we disregard this possibility as it vanishes for zero contact angle [13]. Indeed, there is strong evidence indicating that the wetting is perfect: first, perfect wetting always occurs in the vicinity of the critical point [21]. In addition, we

have measured the equilibrium meniscus height between SF_6 and the glass for a large range of temperature and it coincides with the expected value with zero contact angle. We therefore consider that the additional dissipation measured in this experiment results from viscous loss in (or close to) the meniscus and also scales as $\sqrt{\nu\omega}$.

A power law also describes the behavior of the nonlinear term: $C_{\mathrm{NL}}^{\Delta X} = (647 \pm 17)\epsilon^{0.972\pm0.007}$ mm^{-2} (see Fig. 5). The critical law of C_{NL} follows from

$$C_{\mathrm{NL}} \propto C_{\mathrm{NL}}^{\Delta X}\left(\frac{\Delta X}{\bar{\eta}}\right)^2 \propto C_{\mathrm{NL}}^{\Delta X}\left(\frac{\omega_{1,1}}{Q}\frac{1}{\omega_{1,1}\Delta\rho}\right)^2, \quad (13)$$

that gives $C_{\mathrm{NL}} \propto \epsilon^{0.160\pm0.007}$. This exponent turns out to be very close to $\delta^{-2} \propto \epsilon^{\beta/2}$ ($\beta/2 \simeq 0.1625$), and the equation of this oscillator (5) can finally be cast in the form

$$\frac{\mathrm{d}^2\bar{\eta}_{1,1}}{\mathrm{d}t^2} + \frac{\omega_{1,1}}{Q}\left(1 + C\left(\frac{\bar{\eta}_{1,1}}{\delta}\right)^2\right)\frac{\mathrm{d}\bar{\eta}_{1,1}}{\mathrm{d}t} + \omega_{1,1}^2\bar{\eta}_{1,1} = \mathcal{F}(t), \quad (14)$$

where C is a dimensionless constant that does not depend on ϵ. This proves that linear damping correctly describes sloshing as long as the oscillation amplitudes remain small compared to the thickness of the boundary layer. This result is quite surprising: one could have guessed this crossover length scale to be the size of the meniscus (the so-called capillary length) or the wavelength of the wave, the steepness ($k_{1,1}\bar{\eta}_{1,1}$) characterizing nonlinear coupling between modes [22, 23]. For a perfect wetting and using octane and air instead of SF_6, Cocciaro et al. reported a decrease of the dissipation as the forcing increases [5]. This shows that the nonlinearity observed here does not result from the dynamics of the bottom, top and lateral boundary layers, identical in both experiments. In contrast, a specificity of the present experiment is that energy dissipation occurs both in the liquid and in the gas: since the fluid motions are similar in these two phases except in the vicinity of the contact line, we propose this nonlinear damping to also result from viscous dissipation in or close to the meniscus.

Conclusion.— Our experiment sheds light on two aspects of sloshing theory in perfect wetting. First, it shows that linear damping can reasonably be assumed as long as the oscillation amplitude remains small compared to the thickness of the boundary layer $\delta = \sqrt{\nu/\omega}$. This characteristic length is very small and is quickly exceeded in practice. For this reason, we emphasize the importance of measurements of decay up to very small displacements in experiments dealing with sloshing. Second, we found that damping is underestimated if only viscous boundary layers are considered: a substantial dissipation arises as a consequence of the contact line motion. The study of wetting in nonsteady states represents a substantial experimental and theoretical challenge and our results point out its relevance for sloshing.

* guillaume.michel@ens.fr

[1] S. D. Poisson, Mémoire sur les petites oscillations de leau contenue dans un cylindre, *Annales de mathématiques pures et appliquées*, **19**, 225 (1828).

[2] R. A. Ibrahim, Liquid Sloshing Dynamics (Cambridge University Press, New York, 2005).

[3] H. C. Mayer and R. Krechetnikov, Walking with coffee: Why does it spill?, *Phys. Rev. E*, **85**, 046117 (2012).

[4] H. Lamb, Hydrodynamics (Dover, New York, 1945).

[5] B. Cocciaro, S. Faetti and M. Nobili, Capillarity effects on surface gravity waves in a cylindrical container: wetting boundary conditions, *J. Fluid Mech.*, **231**, 325 (1991).

[6] B. Cocciaro, S. Faetti and C. Festa, Experimental investigation of capillarity effects on surface gravity waves : non-wetting boundary conditions, *J. Fluid Mech.*, **246**, 43 (1993).

[7] K. M. Case and W. C. Parkinson, Damping of surface waves in an incompressible liquid, *J. Fluid Mech.*, **2**, 172 (1956).

[8] D. M. Henderson and J. W. Miles, Surface-wave damping in a circular cylinder with a fixed contact line, *J. Fluid Mech.*, **275**, 285 (1994).

[9] D. R. Howell, B. Buhrow, T. Heath, C. McKenna, W. Hwang and M. F. Schatz, Measurements of surface-wave damping in a container, *Phys. Fluids*, **12**, 322 (2000).

[10] W. G. Van Dorn, Boundary dissipation of oscillatory waves, *J. Fluid Mech.*, **24**, 769 (1966).

[11] J. W. Miles, Surface-Wave Damping in Closed Basins, *Proc. R Soc. Lond. A*, **297**, 459 (1967).

[12] J. A. Nicolás and J. M. Vega, A note on the effect of surface contamination in water wave damping, *J. Fluid Mech.*, **410**, 367 (2000).

[13] J. W. Miles, On surface waves with zero contact angle, *J. Fluid Mech.*, **245**, 485 (1992).

[14] G. Michel, F. Pétrélis, S. Fauve, Acoustic Measurement of Surface Wave Damping by a Meniscus, *Phys. Rev. Lett.*, **116**, 174301 (2016).

[15] D. Henderson, J. Hammack, P. Kumar and D. Shah, The effects of static contact angles on standing waves, *Phys. Fluids A*, **4**, 2320 (1992).

[16] S. N. Biswas, N. Trappeniers and J. Hoogland, PVT Properties of sulfur-hexafluoride in the gaz-liquid critical region,*Physica A*, **126**, 384 (1984).

[17] E. S. Wu and W. W. Webb, Critical liquid-vapor interface in SF6. II. Thermal excitations, surface tension, and viscosity, *Phys. Rev. A*, **8**, 2077 (1973).

[18] Note that close to the resonance, $\Delta X \omega^2 \simeq \Delta X \omega_{1,1}^2$ since the quality factor Q is large compared to unity.

[19] M. R. Moldover, Interfacial tension of fluids near critical points and two-scale-factor universality, *Phys. Rev. A*, **31**, 1022 (1985).

[20] C. Martel, J. A. Nicolás, J. M. Vega, Surface-wave damping in a brimful circular cylinder, *J. Fluid Mech.*, **360**, 213 (1998).

[21] J. W. Cahn, Critical point wetting, *J. Chem. Phys.*, **66**, 3667 (1977).

[22] J. W. Miles, Internally resonant surface waves in a circular cylinder, *J. Fluid Mech.*, **149**, 1 (1984).

[23] J. W. Miles, Resonantly forced surface waves in a circular cylinder, *J. Fluid Mech.*, **149**, 15 (1984).